CRYSTAL GROWTH & DESIGN
2008
VOL. 8, NO. 6
1932–1939

Topological Diversity of Coordination Polymers Containing the Rigid Terephthalate and a Flexible N,N′-Type Ligand: Interpenetration, Polyrotaxane, and Polythreading

Guan-Hua Wang,[†,‡] Zhi-Gang Li,[†,‡] Heng-Qing Jia,[†] Ning-Hai Hu,*[,†] and Jing-Wei Xu*[,†]

Changchun Institute of Applied Chemistry, Chinese Academy of Sciences, Changchun 130022, P. R. China, and Graduate School, Chinese Academy of Sciences, Beijing 100039, P. R. China

Received December 16, 2007; Revised Manuscript Received February 24, 2008

ABSTRACT: Reactions of zinc(II) or cadmium(II) salts with terephthalic acid (H_2tp) and 1,3-bis(4-pyridyl)propane (bpp) have afforded four coordination polymers at room temperature, $[Zn(\mu\text{-tp})(\mu\text{-bpp})]_n \cdot 2nH_2O$ (**1**), $[Cd_2(\mu\text{-tp})_2(\mu\text{-bpp})_3]_n \cdot 2nH_2O$ (**2**), $[Cd(\mu\text{-tp})(\mu\text{-bpp})(H_2O)]_n \cdot nH_2O$ (**3**), and $[Cd_2(\mu\text{-tp})(\mu\text{-bpp})_2(bpp)_2Br_2]_n$ (**4**). Single-crystal X-ray diffraction has revealed interesting topological features for these compounds. In **1**, the Zn atoms act as 4-connected nodes bridged by the tp and bpp ligands to give a 3-fold interpenetrated 3D network with a unique 6^6 topology, which is evidently distinct from 4-connected diamondoid networks. **2** represents the first example of a 2-fold interpenetrated coordination polymer, which possesses a 5-connected 3D framework with a unique 6^{10} topology constructed from Cd nodes and tp and bpp spacers. **3** manifests a polyrotaxane motif comprised of two interlocked sets of identical sheets, which result in a 2D → 2D polythreaded layer. Parallel mutual polythreading of 2D layers with dangling bpp ligands is observed in **4**, involving five polymeric layers at a time and thus affording a 3D architecture. All compounds were characterized by infrared spectroscopy, elemental analysis, thermogravimetric analysis, and their fluorescence properties were also investigated.

Introduction

During the past decade, the design and construction of coordination polymers have attracted much attention because of their intriguing structural topologies and various potential applications, including catalysis, nonlinear optics, sensors, magnetism and molecular recognition.[1] Intelligent design of ligands and proper choice of metal centers are the main keys to the designing of intriguing and useful coordination polymers. However, predicting the final supramolecular framework constructed by a set of ligands and metal centers is often difficult because it can be affected by many factors, such as coordination activities of the metal centers, nature of the ligands used, metal–ligand ratio, nature of the counteranions, and various experimental conditions.[2] Experimental net-based approach to the construction of coordination polymers has provided a useful tool for design of new materials.[3]

Many coordination networks are particularly intriguing because of the presence of periodic entanglements, in which independent motifs are entangled together in different ways. Among different types of entanglements, interpenetrating networks have been extensively studied.[4] In recent years, the intense interest in coordination polymers has led to more topological types of entanglements being discovered, such as polycatenation, polythreading, and polyknotting. According to Carlucci, Ciani, and Proserpio,[5] interpenetration is one of the subclasses of entangled systems. It represents the entanglement between a limited number of motifs with identical topology, in which each motif is interlaced with all the other ones. Polycatenation is differentiated from interpenetration in that the component motifs have lower dimensionality than that of the resulting architectures and that each individual motif is catenated only with the surrounding ones not with all the others. Polythreading can be used to describe a type of entanglements that feature closed loops and rod or string elements that can thread through the loops. The known polythreaded systems can be distinguished into two classes:[5a] in one class of the systems, the so-called "polyrotaxane", the different motifs cannot be disentangled without breaking links, and the other class of the systems contain "separable" motifs. Undoubtedly, the exploitation of entangled structures can be helpful not only for both the design and analysis of crystal structures but also for understanding the relationships between the structure and function of these coordination polymers.

To design coordination polymers with interesting structure and excellent performance, the match of metal centers with suitable ligands and synergistic effects of the ligands are crucial factors.[6] An effective strategy is using one ligand to construct basic units and another auxiliary ligand to extend the framework.[7] Utilizing Zn(II) and Cd(II) ions as nodes and a rigid tp ligand and a flexible bpp ligand as spacers, we have obtained four new entangled complexes with interesting topologies, $[Zn(\mu\text{-tp})(\mu\text{-bpp})]_n \cdot 2nH_2O$ (**1**) (H_2tp = terephthalic acid; bpp = 1,3-bis(4-pyridyl)propane) and $[Cd_2(\mu\text{-tp})_2(\mu\text{-bpp})_3]_n \cdot 2nH_2O$ (**2**) are the first examples of 3- and 2-fold interpenetrating networks with unique 6^6 and 6^{10} topologies, respectively. $[Cd(\mu\text{-tp})(\mu\text{-bpp})(H_2O)]_n \cdot nH_2O$ (**3**) is a two-dimensional (2D) polyrotaxane net and $[Cd_2(\mu\text{-tp})(\mu\text{-bpp})_2(bpp)_2Br_2]_n$ (**4**) is a polythreaded system arising from 2D (6, 3) nets with long dangling arms. In this paper, a convenient method at room temperature was employed to prepare this family of complexes.

Experimental Section

Materials and General Methods. The reagents and solvents employed were commercially available and used as received without further purification. The IR spectra were recorded from KBr pellets on a Bruker VERTEX70 FTIR spectrometer in the 400−4000 cm^{-1} region. The C, H, and N microanalyses were carried out on a Vario EL elemental analyzer. Fluorescent spectra were measured with a HITACHI F-4500 fluorescence spectrophotometer. Thermogravimetric analysis was performed on a Perkin-Elmer TGA7 thermal analyzer under flowing N_2 with a heating rate of 10 °C min^{-1} between 40 and 700 °C.

* Corresponding author. Tel: 86-431-85262342. Fax: 86-431-85685653. E-mail: hunh@ciac.jl.cn.
† Changchun Institute of Applied Chemistry, Chinese Academy of Sciences.
‡ Graduate School, Chinese Academy of Sciences.

10.1021/cg701232n CCC: $40.75
Published on Web 05/13/2008

Table 1. Crystal Data and Structure Refinements for 1–4

	1	2	3	4
formula	$C_{21}H_{22}N_2O_6Zn$	$C_{55}H_{54}Cd_2N_6O_{10}$	$C_{21}H_{22}CdN_2O_6$	$C_{60}H_{60}Br_2Cd_2N_8O_4$
fw	463.78	1183.84	510.81	1341.78
cryst syst	monoclinic	orthorhombic	triclinic	monoclinic
space group	*C*2/*c*	*Pbca*	$P\bar{1}$	$P2_1/c$
a (Å)	9.4758(1)	17.5805(10)	8.670(2)	13.2305(9)
b (Å)	17.8003(12)	18.0403(10)	10.028(2)	15.2743(10)
c (Å)	25.6003(17)	32.8141(18)	12.476(3)	13.9145(9)
α (deg)	90.00	90.00	74.158(3)	90.00
β (deg)	97.299 (1)	90.00	78.893(3)	99.249(1)
γ (deg)	90.00	90.00	89.453(3)	90.00
V(Å^3)	4283.1(5)	10407(1)	1022.9(4)	2775.4(3)
Z	8	8	2	2
D_{calcd} (g cm^{-3})	1.438	1.511	1.658	1.606
μ (mm^{-1})	1.186	0.882	1.108	2.261
T (K)	187(2)	187(2)	293(2)	187(2)
θ_{max} (deg)	25.19	25.38	25.99	26.06
no. of reflns collected	11915	53806	5409	15319
no. of unique reflns	4238	9683	3625	5463
R_{int}	0.0280	0.0646	0.0125	0.0158
GOF	1.042	1.016	1.030	1.036
R1 [$I > 2\sigma(I)$][a]	0.0377	0.0458	0.0239	0.0304
wR2 (all data)[b]	0.0998	0.1028	0.0616	0.0799

[a] $R1 = \Sigma| |F_o| - |F_c| |/\Sigma|F_o|$. [b] $wR2 = [\ \Sigma w(F_o^2 - F_c^2)^2/\Sigma w(F_o^2)^2]^{1/2}$.

Synthesis of [Zn(*μ*-tp)(*μ*-bpp)]$_n$·2*n*H$_2$O (1). A solution of $Zn(ClO_4)_2 \cdot 6H_2O$ (0.186 g, 0.5 mmol) in H_2O (4 mL) was added to a suspending solution of H_2tp (0.083 g, 0.5 mmol) in H_2O (7 mL), followed by dropwise addition of a solution of bpp (0.059 g, 0.3 mmol) in DMF (3 mL). Aqueous NH_3 (25%, 0.06 mL) was then slowly added to the reaction mixture, making sure that the pH value is 7−8. The resulting solution was filtered off. Colorless crystals were obtained by allowing the filtrate to stand at room temperature for 3 days. Yield: 0.144 g (62% based on Zn). Anal. Calcd for $C_{21}H_{22}N_2O_6Zn$: C, 54.39; H, 4.78; N, 6.04. Found: C, 54.22; H, 4.73; N, 6.01. IR (KBr, cm^{-1}): 3467 (s, br), 2933 (vw), 2868 (vw), 1622 (s), 1593 (s), 1502 (m), 1433 (m), 1366 (s), 1225 (w), 1069 (w), 1031 (w), 832 (m), 751 (s), 578 (m), 523 (m).

Synthesis of [Cd$_2$(*μ*-tp)$_2$(*μ*-bpp)$_3$]$_n$·2*n*H$_2$O (2). The procedure is similar to the synthesis of **1** except that $Cd(NO_3)_2 \cdot 4H_2O$ (0.154 g, 0.5 mmol) was used instead of $Zn(ClO_4)_2 \cdot 6H_2O$. Yield: 0.161 g (54%). Anal. Calcd for $C_{55}H_{54}Cd_2N_6O_{10}$: C, 55.80; H, 4.60; N, 7.10. Found: C, 55.19; H, 4.23; N, 7.13. IR (KBr, cm^{-1}): 3441 (s, br), 3063 (w), 2935 (w), 1949 (vw), 1613 (s), 1571 (s), 1501 (m), 1426 (m), 1386 (s), 1223 (m), 1071 (w), 1015 (s), 835 (m), 753 (s), 508 (w).

Synthesis of [Cd(*μ*-tp)(*μ*-bpp)(H$_2$O)]$_n$·*n*H$_2$O (3). The procedure is similar to the synthesis of **1** except that $Cd(CH_3COO)_2 \cdot 2H_2O$ (0.133 g, 0.5 mmol) was used instead of $Zn(ClO_4)_2 \cdot 6H_2O$. Yield: 0.242 g (71%). Anal. Calcd for $C_{21}H_{22}CdN_2O_6$: C, 49.38; H, 4.34; N, 5.48. Found: C, 49.25; H, 4.29; N, 5.45. IR (KBr, cm^{-1}): 3449 (s, br), 2934 (vw), 1613 (m), 1562 (s), 1502 (m), 1426 (m), 1386 (s), 1224 (w), 1071 (w), 1015 (m), 839 (m), 752 (s), 520 (w).

Synthesis of [Cd$_2$(*μ*-tp)(*μ*-bpp)$_2$(bpp)$_2$Br$_2$]$_n$ (4). The procedure is similar to the synthesis of **1** except that $Cd(Br)_2 \cdot 4H_2O$ (0.172 g, 0.5 mmol) was used instead of $Zn(ClO_4)_2 \cdot 6H_2O$. Yield: 0.138 g (58%). Anal. Calcd for $C_{60}H_{60}Br_2Cd_2N_8O_4$: C, 53.71; H, 4.51; N, 8.35. Found: C, 53.56; H, 4.45; N, 8.32. IR (KBr, cm^{-1}): 3431 (s, br), 2930 (w), 2862 (vw), 1611 (s), 1563 (s), 1548 (s), 1503 (m), 1425 (m), 1381 (s), 1227 (m), 1072 (w), 1014 (m), 836 (m), 813 (m), 751 (m), 609 (w), 515 (m).

Caution! *Metal perchlorates can be explosive. They should be handled only with great care and in small quantities.*

X-ray Crystallography. Single-crystal X-ray diffraction measurements were carried out on a Bruker SMART APEX CCD diffractometer equipped with graphite-monochromated Mo Kα radiation (λ = 0.71073 Å). Absorption corrections were applied using SADABS program.[8] The structures were solved by direct methods and refined on F^2 using full-matrix least-squares methods (SHELXS97 and SHELXL97 programs).[9] All non-hydrogen atoms were refined anisotropically. Hydrogen atoms attached to carbon atoms were positioned geometrically and refined as riding atoms with $U_{iso}(H) = 1.2U_{eq}(C)$. Hydrogen atoms of water molecules were located in difference Fourier maps and fixed in the refinements. Crystallographic data and experimental details for **1**−**4** are summarized in Table 1. Selected bond lengths and angles are listed in Table 2.

Results and Discussion

Effects of the Ligands and Metal Salts on Structural Motifs. Polycarboxylates are often employed as bridging ligands to construct porous coordination polymers, due to their versatile coordination modes and high structural stability.[1e,10] The bpp molecule can adopt four types of conformations including *TT*, *TG*, *GG*, and *GG′* (considering the relative orientations of the three CH_2 groups, *T* = trans, *G* = gauche).[11] As 4,4′-bipyridine analogue, bpp has proven to be a good candidate for the construction of interpenetrating systems because of its length and flexibility. In this work, reactions of the tp and bpp ligands with different metal sources afford four entirely different structural motifs, presumably due to the nature of metal salts. The use of $Zn(ClO_4)_2$ provided a 3-fold interpenetrating network (**1**). When employing different $Cd(X)_2$ salts, a 2-fold interpenetrating network (**2**) ($X = NO_3^-$), a 2D polyrotaxane layer (**3**) ($X = CH_3COO^-$) and a polythreading motif (**4**) ($X = Br^-$) were obtained. Our experiments indicated that the products were not affected by both the changes of mole ratio and solvent, which supports the fact that anions may play a directing role in the formation of different structural motifs, although they do not participate in the structure construction in the cases of **1**−**3**. The absence of IR absorption bands around 1700 cm^{-1}, attributed to protonated carboxyl group, indicates the full deprotonation of the tp ligands in **1**−**4**, as revealed by the single-crystal structure analysis. The strong peaks at 1593 and 1366 cm^{-1} for **1**, 1571 and 1386 cm^{-1} for **2**, 1562 and 1386 cm^{-1} for **3**, 1563 and 1381 cm^{-1} for **4** correspond to υ_{asym} and υ_{sym} of the coordinated carboxylate groups, respectively. All the products are insoluble in water and common organic solvents.

Crystal Structure of [Zn(*μ*-tp)(*μ*-bpp)]$_n$·2*n*H$_2$O (1). A single-crystal X-ray diffraction study reveals that complex **1** crystallizes in the monoclinic space group *C*2/*c* and features a 3-fold interpenetrating 3D framework. The asymmetric unit of **1** contains a four-coordinated Zn(II) atom, two halves of tp ligands, one bpp ligand and two free water molecules. Each Zn atom is coordinated in a distorted tetrahedral geometry (Figure 1a), which is defined by two O atoms from the monodentate carboxylate groups of two tp ligands (Zn−O = 1.948(2) and 1.954(2) Å) and two N atoms from two bpp ligands (Zn−N = 2.024(2) and 2.042(2) Å). The bond angles at the Zn atom are in a range of 101.17(8)−119.51(8)°, in accord with the values

Table 2. Selected Bond Lengths (Å) and Angles (deg) for 1−4

				1[a]			
Zn(1)−O(3)	1.948(2)	Zn(1)−O(1)	1.954(2)	Zn(1)−N(1)	2.024(2)	Zn(1)−N(2a)	2.042(2)
O(3)−Zn(1)−O(1)	101.17(8)	O(3)−Zn(1)−N(1)	119.51(8)	O(1)−Zn(1)−N(1)	117.06(8)	O(3)−Zn(1)−N(2a)	103.37(8)
O(1)−Zn(1)−N(2a)	103.75(8)	N(1)−Zn(1)−N(2a)	110.05(8)				
				2[b]			
Cd(1)−O(1)	2.306(3)	Cd(1)−O(3)	2.309(3)	Cd(1)−N(3)	2.309(3)	Cd(1)−N(6a)	2.372(4)
Cd(1)−N(1)	2.412(4)	Cd(1)−O(2)	2.532(3)	Cd(1)−O(4)	2.582(3)	Cd(2)−O(8)	2.296(3)
Cd(2)−O(6)	2.315(3)	Cd(2)−N(4b)	2.347(4)	Cd(2)−N(2c)	2.382(4)	Cd(2)−N(5)	2.384(4)
Cd(2)−O(7)	2.533(3)	Cd(2)−O(5)	2.569(3)				
O(1)−Cd(1)−O(3)	83.85(10)	O(1)−Cd(1)−N(3)	136.03(11)	O(3)−Cd(1)−N(3)	139.84(11)	O(1)−Cd(1)−N(6a)	94.32(12)
O(3)−Cd(1)−N(6a)	83.47(12)	N(3)−Cd(1)−N(6a)	95.51(12)	O(1)−Cd(1)−N(1)	87.40(12)	O(3)−Cd(1)−N(1)	90.69(11)
N(3)−Cd(1)−N(1)	87.39(12)	N(1)−Cd(1)−N(6a)	173.69(12)	O(1)−Cd(1)−O(2)	53.70(10)	O(3)−Cd(1)−O(2)	136.72(10)
N(3)−Cd(1)−O(2)	83.36(10)	O(2)−Cd(1)−N(6a)	90.97 (11)	N(1)−Cd(1)−O(2)	94.94(11)	O(1)−Cd(1)−O(4)	136.81(10)
O(3)−Cd(1)−O(4)	53.50(9)	N(3)−Cd(1)−O(4)	86.34(11)	O(4)−Cd(1)−N(6a)	87.91(11)	N(1)−Cd(1)−O(4)	86.69(11)
O(2)−Cd(1)−O(4)	169.49(9)	O(8)−Cd(2)−O(6)	89.62(11)	O(8)−Cd(2)−N(4b)	139.65(11)	O(6)−Cd(2)−N(4b)	130.53(12)
O(8)−Cd(2)−N(2c)	87.17(12)	O(6)−Cd(2)−N(2c)	97.10(12)	N(4b)−Cd(2)−N(2c)	90.83(12)	O(8)−Cd(2)−N(5)	97.04(12)
O(6)−Cd(2)−N(5)	87.92(12)	N(5)−Cd(2)−N(4b)	82.75(12)	N(5)−Cd(2)−N(2c)	173.49(12)	O(8)−Cd(2)−O(7)	54.17(10)
O(6)−Cd(2)−O(7)	143.02(11)	O(7)−Cd(2)−N(4b)	85.52(11)	O(7)−Cd(2)−N(2c)	89.14(12)	N(5)−Cd(2)−O(7)	89.31(12)
O(8)−Cd(2)−O(5)	139.22(11)	O(6)−Cd(2)−O(5)	53.43(11)	O(5)−Cd(2)−N(4b)	79.92(11)	O(5)−Cd(2)−N(2c)	81.85(11)
N(5)−Cd(2)−O(5)	97.98(11)	O(7)−Cd(2)−O(5)	162.72(11)				
				3[c]			
Cd(1)−O(1W)	2.298(2)	Cd(1)−N(2a)	2.366(2)	Cd(1)−N(1)	2.384(2)	Cd(1) −O(2)	2.387(2)
Cd(1)−O(3)	2.392(2)	Cd(1)−O(1)	2.437(2)	Cd(1)−O(4)	2.518(2)		
O(5)−Cd(1)−N(2a)	85.46(7)	O(1W)−Cd(1)−N(1)	178.68(7)	N(1)−Cd(1)−N(2a)	95.84(7)	O(1W)−Cd(1)−O(2)	92.40(8)
O(2)−Cd(1)−N(2a)	84.80(7)	N(1)−Cd(1)−O(2)	87.98(8)	O(1W)−Cd(1)−O(3)	90.65(7)	O(3)−Cd(1)−N(2a)	136.00(6)
N(1)−Cd(1)−O(3)	88.24(7)	O(2)−Cd(1)−O(3)	139.20(6)	O(1W)−Cd(1)−O(1)	89.31(7)	O(1)−Cd(1)−N(2a)	138.23(7)
N(1)−Cd(1)−O(1)	89.89(7)	O(2)−Cd(1)−O(1)	54.01(6)	O(3)−Cd(1)−O(1)	85.37(6)	O(1W)−Cd(1)−O(4)	92.89(7)
O(4)−Cd(1)−N(2a)	83.27(6)	N(1)−Cd(1)−O(4)	87.02(7)	O(2)−Cd(1)−O(4)	166.52(6)	O(3)−Cd(1)−O(4)	53.12(6)
O(1)−Cd(1)−O(4)	138.44(6)						
				4[d]			
Cd(1)−N(2a)	2.343(2)	Cd(1)−O(2)	2.370(2)	Cd(1)−N(3)	2.377(2)	Cd(1)−N(1)	2.394(2)
Cd(1)−O(1)	2.430(2)	Cd(1)−Br(1)	2.631(4)				
O(2)−Cd(1)−N(2a)	83.78(7)	N(3)−Cd(1)−N(2a)	88.97(8)	O(2)−Cd(1)−N(3)	87.51(8)	N(1)−Cd(1)−N(2a)	92.95(8)
O(2)−Cd(1)−N(1)	88.52(8)	N(3)−Cd(1)−N(1)	175.38(8)	O(1)−Cd(1)−N(2a)	138.56(7)	O(2)−Cd(1)−O(1)	54.90(7)
N(3)−Cd(1)−O(1)	91.86(7)	N(1)−Cd(1)−O(1)	83.92(7)	Br(1)−Cd(1)−N(2a)	102.75(5)	O(2)−Cd(1)−Br(1)	173.38(5)
N(3)−Cd(1)−Br(1)	91.44(6)	N(1)−Cd(1)−Br(1)	92.23(6)	O(1)−Cd(1)−Br(1)	118.63(5)		

[a] See Figure 1 for symmetry codes. [b] See Figure 3 for symmetry codes. [c] See Figure 5 for symmetry codes. [d] See Figure 7 for symmetry codes.

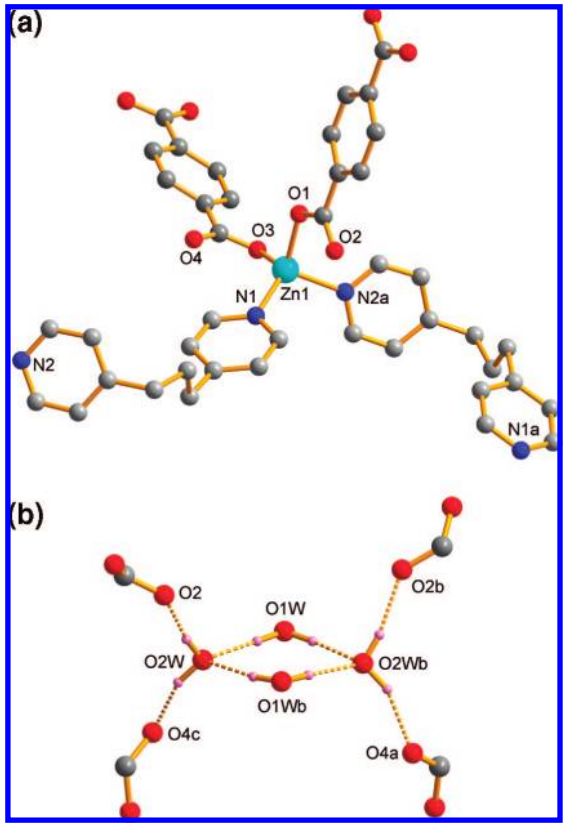

Figure 1. (a) View of the coordination environment of the Zn(II) atom in **1**. (b) Water tetramer lying in the channel of **1**, showing the configuration of the tetramer. Dashed lines denote hydrogen bonds. Symmetry codes: $a = 1.5 - x, y - 0.5, 1.5 - z$; $b = 2 - x, y, 1.5 - z$; $c = 0.5 + x, y - 0.5, z$.

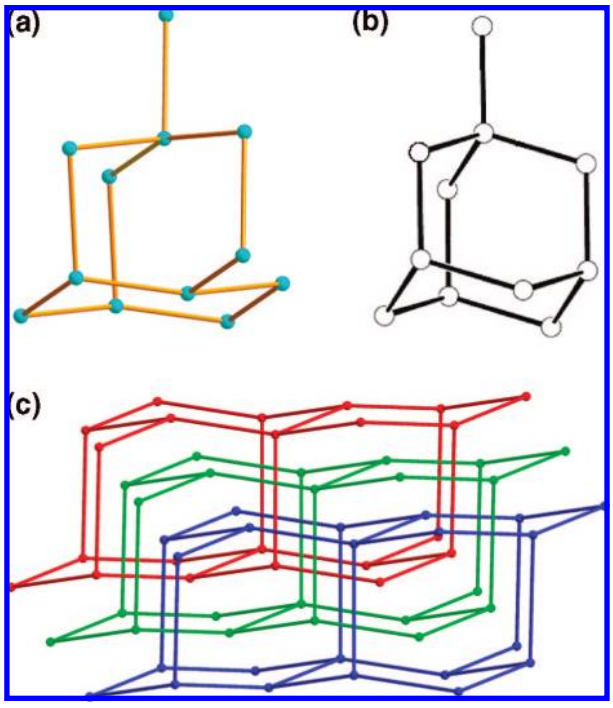

Figure 2. A comparison of a basic unit (a) from the network of **1** and an adamantane unit (b) from diamondoid network. (c) A schematic view of the 3-fold interpenetration of $6{\cdot}6{\cdot}6{\cdot}6_2{\cdot}6_2{\cdot}6_2$ nets in **1**.

for a tetrahedral geometry. The tp ligands bind to Zn atoms in a bis-monodentate bridging mode. The bpp ligand adopts the

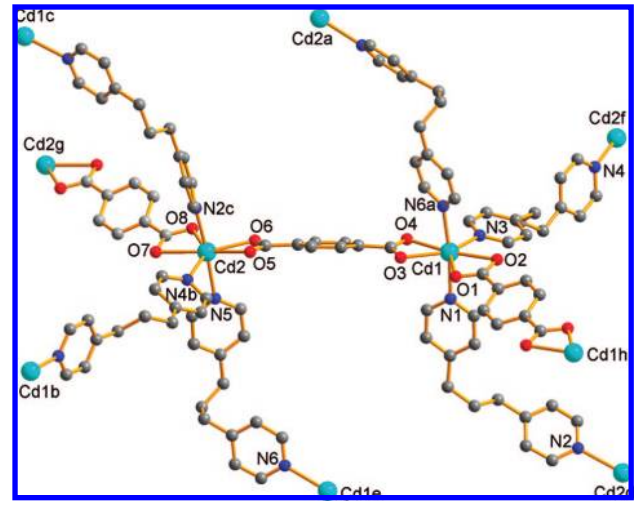

Figure 3. Coordination environments of the Cd(II) atoms in **2**. Symmetry codes: $a = -0.5 + x, y, 1.5 - z$; $b = 0.5 + x, 1 + y, 1.5 - z$; $c = -0.5 + x, 1 + y, 1.5 - z$; $d = 0.5 + x, -1 + y, 1.5 - z$; $e = 0.5 + x, y, 1.5 - z$; $f = -0.5 + x, -1 + y, 1.5 - z$; $g = -x, 1 - y, 2 - z$; $h = 1 - x, -y, 1 - z$.

TG conformation, with an N···N distance of 8.32 Å and a dihedral angle of 54.0° between two pyridyl rings. If considering that each Zn atom is connected by one tp and two bpp ligands, the extension of these nodes leads to a (6, 3) sheet. The other tp ligand is further linked to the Zn atom to complete a 4-connected node, which extends the (6, 3) sheets into a 3D framework with a 6^6 topology. This type of topology is interesting as the 4-connected nodes with a tetrahedral geometry usually result in diamondoid networks.[12] The complex **1**, however, represents a rarely observed 4-connected net with a long Schläfli symbol $6{\cdot}6{\cdot}6{\cdot}6_2{\cdot}6_2{\cdot}6_2$, which is different from the symbol $6_2{\cdot}6_2{\cdot}6_2{\cdot}6_2{\cdot}6_2{\cdot}6_2$ for the diamondoid net.[13] Figure 2 gives a comparison of basic units from the two nets.

In **1**, the (6, 3) sheets are pillared by the tp ligands, thus resulting in a large hexagonal channel of approximately 15.0 × 13.6 Å, which allows each net to be penetrated by two other independent nets (Figure 2c). To our knowledge, this is the first example of a 3-fold interpenetration network with $6{\cdot}6{\cdot}6{\cdot}6_2{\cdot}6_2{\cdot}6_2$ topology. The PLATON calculation[14] shows that the compound still retains an effective void volume of 562.7Å^3 per unit cell upon interpenetration, which corresponds to 13.1% of the crystal volume. Interestingly, hydrogen-bonded tetrameric water clusters exist in the channel along the [100] direction. In the water tetramer (Figure 1b), O1W and its symmetric equivalent act as hydrogen-bonding donors and O2W and its symmetric equivalent as acceptors. Moreover, O2W also serves as hydrogen-bonding donors to adjacent carboxylate O atoms from the tp ligands. Thus the configuration of the water tetramer is different from the commonly observed udud and uudd forms.[15]

Crystal Structure of $[Cd_2(\mu\text{-tp})_2(\mu\text{-bpp})_3]_n{\cdot}2nH_2O$ (2). Complex **2** crystallizes in the orthorhombic space group *Pbca* and exhibits a 2-fold interpenetrating 3D framework. The asymmetric unit contains two Cd(II) atoms (Cd1 and Cd2), one and two halves of tp ligands, three bpp ligands, and two free water molecules. Each Cd atom is seven-coordinated in a distorted pentagonal-bipyramidal geometry (Figure 3), which is composed of one N atom from a bpp ligand and four O atoms from two chelate carboxylate groups of two tp ligands in the equatorial plane, and two N atoms from the two other bpp ligands in the axial positions. The tp ligands are coordinated to Cd atoms in

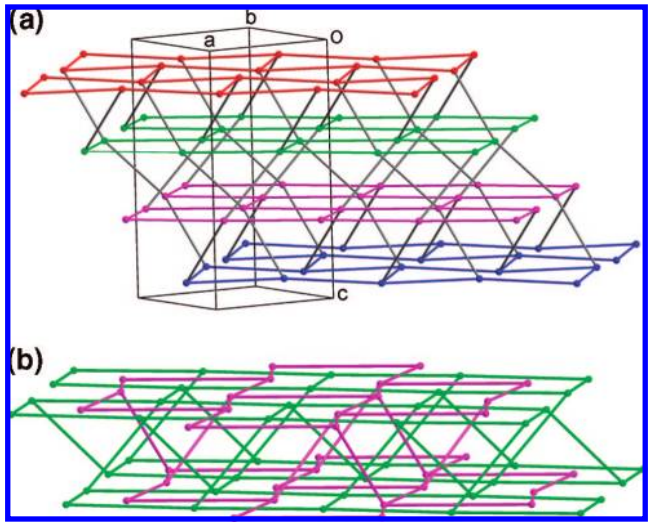

Figure 4. (a) Single 5-connected 3D net in **2**, which is constructed by tp ligands (gray) pillaring (6, 3) sheets in an ABCD sequence. (b) Schematic view of the 2-fold interpenetrating 6^{10} network.

a bis-chelate bridging mode. One bpp ligand (containing N5 and N6) adopts the *GG* conformation, with an N. . .N distance of 8.35 Å, and the other two assume the *TG* conformation, with N. . .N distances of 9.23 and 9.92 Å. The dihedral angles of two pyridyl rings are 46.1, 69.0, 27.2°, respectively. All the tp and bpp ligands act as bridging spacers to link the Cd nodes into a 3D framework. As shown in Figure 3, the Cd atoms are arranged in a Cd1−Cd1−Cd2−Cd2 sequence when linked by tp ligands, while they are in a Cd1−Cd2 sequence when linked by bpp ligands.

The bpp ligands link Cd atoms into a 2D brick wall network with a (6, 3) topology. As shown in Figure 4a, these (6, 3) sheets are parallely arranged along the *c* direction in an ABCD sequence and the tp ligands join two Cd atoms belonging to two adjacent sheets through the carboxylate coordination. The resulting array is a 5-connected 3D network with a 6^{10} topology. A close inspection revealed that this network has a long Schläfli symbol $6\cdot6_2\cdot6_2\cdot6_3\cdot6_3\cdot6_3\cdot6_3\cdot6_3\cdot6_3\cdot6_4$, evidently different from the previously reported 6^{10} network in a nickel complex,[16] which shows a uniform 6^{10} topology with a long symbol $6_3\cdot6_3\cdot6_3\cdot6_3\cdot6_3\cdot6_3\cdot6_3\cdot6_3\cdot6_3\cdot6_3$. The 5-connected nodes usually result in $4^4\cdot6^6$ and $4^6\cdot6^4$ topologies.[12,17] The present network is the first of its type to the best of our knowledge. Moreover, the interesting structural feature is that two identical 6^{10} nets are entangled to create a 2-fold interpenetrating motif, as illustrated in Figure 4b. After interpenetration, the effective voids are reduced to 536.6 $Å^3$, which is 5.1% of the total volume.

Crystal Structure of $[Cd(\mu\text{-tp})(\mu\text{-bpp})(H_2O)]_n\cdot nH_2O$ (3). Complex **3** crystallizes in the triclinic space group $P\bar{1}$. The asymmetric unit consists of one Cd(II) atom, two halves of tp ligands, one bpp ligand, one coordinated water molecule and one free water molecule. Like that in **2**, the tp ligands adopt a bis-chelate bridging mode. The Cd atom is seven-coordinated in a distorted pentagonal-bipyramidal geometry, defined by one N atom from a bpp ligand and four O atoms from two chelating carboxylate groups of two tp ligands in the equatorial plane, and one bpp N atom and one water molecule in the axial positions (Figure 5a). The bpp ligand in the *TG* conformation presents an N···N distance of 8.58 Å and a dihedral angle of 95.1° between the pyridyl rings.

The most striking structural feature of **3** is a polyrotaxane motif comprised of two interlocked sets of identical sheets,

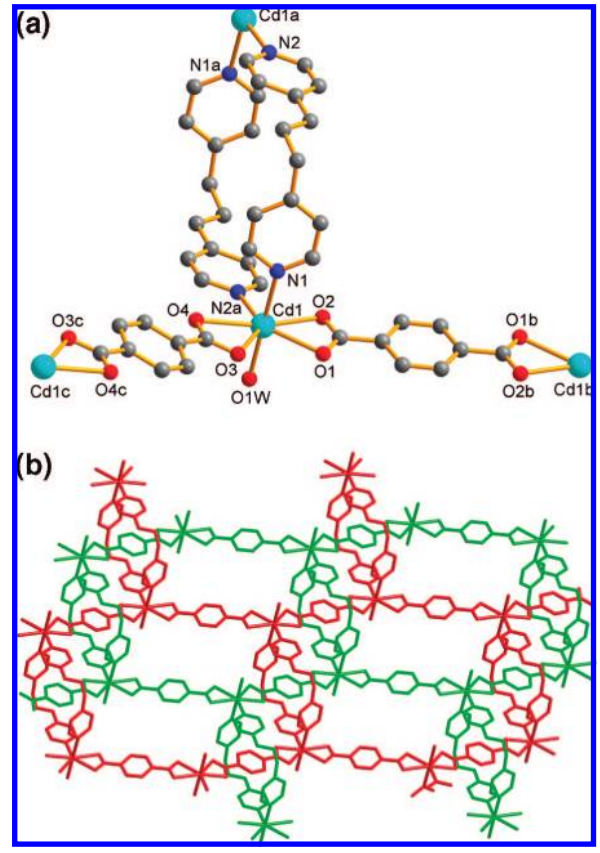

Figure 5. (a) Coordination environment of the Cd(II) atom in **3**. (b) Two interlocked sets of honeycomblike sheets. Symmetry codes: a = $-x, 2-y, 2-z$; b = $2-x, 2-y, 2-z$; c = $1-x, 1-y, 1-z$.

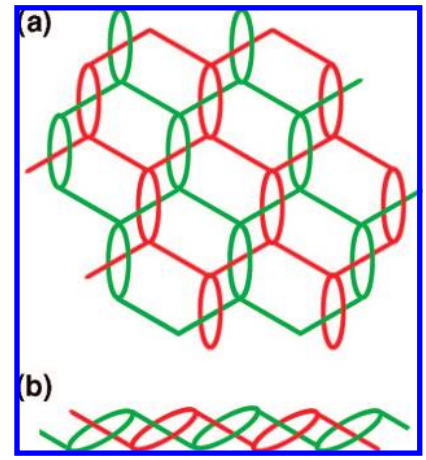

Figure 6. (a) Schematic view of the 2D → 2D polythreaded layer in **3**, which can be viewed as a result of 1D polyrotaxane chains, as shown in (b), linked by rods.

which result in a 2D → 2D polythreaded layer. As seen from Figure 5b, the tp and bpp ligands bridge the Cd atoms to form a 2D honeycomblike sheet, in which each hexagon has four edges represented by the tp ligands and two edges replaced by rings. Each ring is formed by a cyclic $Cd_2(bpp)_2$ unit. Two such honeycomblike sheets interpenetrate as schematically shown in Figure 6a, thus generating a 2D polyrotaxane layer. It is interesting to note that in each sheet all the rings are threaded by rods belonging to the other sheet. This motif can also be viewed as a result of 1D polythreaded chains (see Figure 6b)

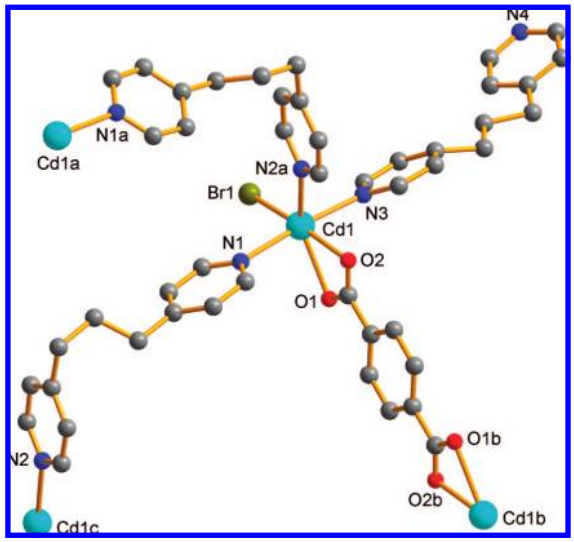

Figure 7. Coordination environment of the Cd(II) atom in **4**. Symmetry codes: $a = -x, 0.5 + y, 0.5 - z$; $b = 1 - x, -y, 1 - z$; $c = -x, -0.5 + y, 0.5 - z$.

linked by the tp rods. The resulting 2D polythreaded layers are stacked along the [0 1 $\bar{1}$] direction and connected by hydrogen bonds between the coordinated water molecules and carboxylate O atoms from adjacent layer. The free water molecules are located in voids (4.9% of the unit-cell volume) between the polythreaded chains.

Polythreaded motifs can be regarded as periodically extended analogues of the molecular rotaxanes. The polythreaded coordination polymers are relatively rare because the systems require the presence of rings and rods that can thread the rings. Two types of polyrotaxane motifs have been reported including 1D → 1D chain,[18] as shown in Figure 6b, and 1D → 2D polythreaded arrays.[19] Up to now, the only known example showing the same 2D → 2D polythreaded array as that of **3** is the complex $[Zn(bix)_2(NO_3)_2]\cdot 4.5H_2O$ (bix = 1,4-bis(imidazol-1-ylmethyl)benzene) reported by Robson and co-workers,[20] in which both the ring and rod elements consist of the flexible bix ligands.

Crystal Structure of $[Cd_2(\mu\text{-tp})(\mu\text{-bpp})_2(bpp)_2Br_2]_n$ (4). Complex **4** crystallizes in the monoclinic space group $P2_1/c$. The asymmetric unit contains one Cd(II) atom, a half of tp ligand, one Br atom and two bpp ligands. The tp ligand adopts the same binding mode as that in **2** and **3**. Different from those in **2** and **3**, however, the Cd atom is six-coordinate in a distorted octahedral geometry. As shown in Figure 7, two O atoms from a chelating carboxylate group, one Br atom and one N atom from a bpp ligand form the equatorial plane and the other two N atoms from two different bpp ligands occupy the axial positions. The Cd−O and Cd−N distances are within the normal range (Table 2). The bpp ligand containing N3 and N4 adopts a unidentate coordination mode with N4 uncoordinated. This type of coordination mode can also be seen in some reported compounds containing bpp ligands.[21] The unidentate dangling bpp ligand has a disordered CH_2CH_2 group and the N···N distance (9.622 Å) is larger than that (8.615 Å) of the μ-bpp ligand containing N1 and N2 atoms. The dihedral angles between the two pyridyl rings are 19.8° for the dangling ligand and 69.3° for the bridging ligand.

Parallel mutual polythreading of 2D layers with dangling arms, affording a 3D architecture, is observed in **4**. As seen in Figure 8a, the Cd centers are bridged by the μ-tp and the μ-bpp

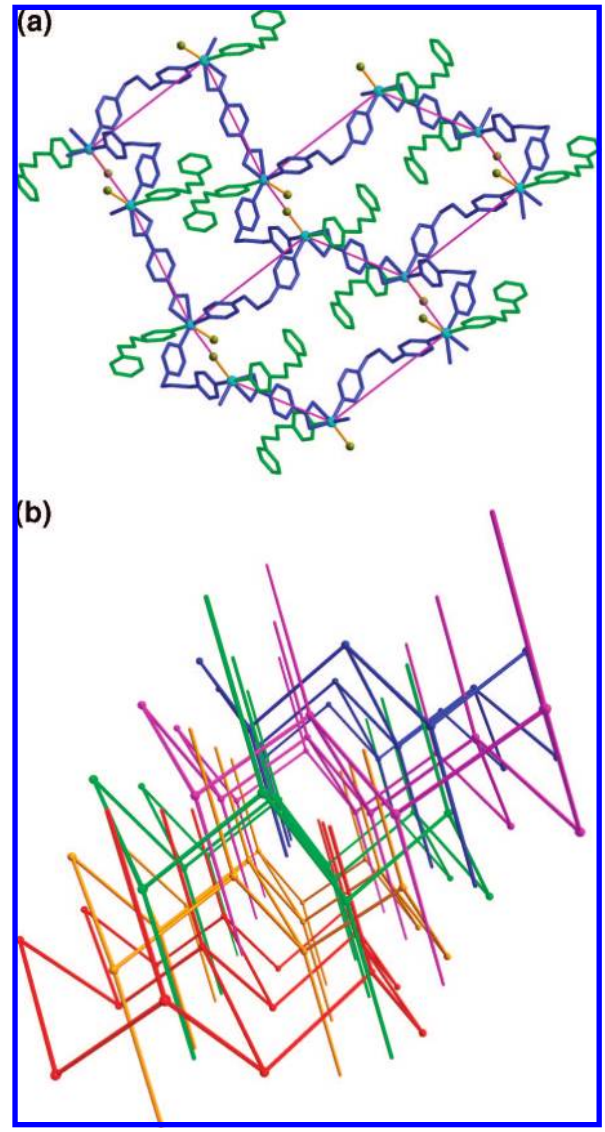

Figure 8. (a) Undulated (6,3) sheet with dangling bpp arms (green) in **4**. (b) Schematic view of the mutual polythreading of five layers.

ligands, leading to the formation of a highly undulated (6, 3) sheet. The six-membered rings composed of Cd centers in the sheet are all in a chair-form with the dangling bpp ligands pointing alternately up and down. The sheets are stacked along the [10$\bar{1}$] direction in an ABC sequence. Each dangling arm has an effectual length of about 11.9 Å so that the arm is able to thread the meshes of two sheets, not only the first but also the second nearest neighboring sheets. As a result, each hexagonal mesh is threaded by four arms from the above and the below, thus resulting in a 2D → 3D polythreading motif involving five polymeric layers at a time (Figure 8b). The threading array is stabilized by π-π interactions between the pridyl rings of the dangling bpp and the bridging bpp ligands, with an interplanar distance of 3.43 Å.

This type of polythreading involving 2D components is still rare according to the literature.[5b] Molecular ladders with dangling arms that lead to 1D → 2D[22] or 1D → 3D[23] by mutual polythreading have been reported. An interesting known example of a 2D→3D polythreading network is the complex $[Ni_3(oba)_2(bpy)_2(Hoba)_2(H_2O)_2]\cdot bpy\cdot 2H_2O$ (oba = 4,4′-oxybis(benzoate) and bpy = 4,4′-bipyridine),[24] in which each 2D layer takes part in interactions with the four nearest layers

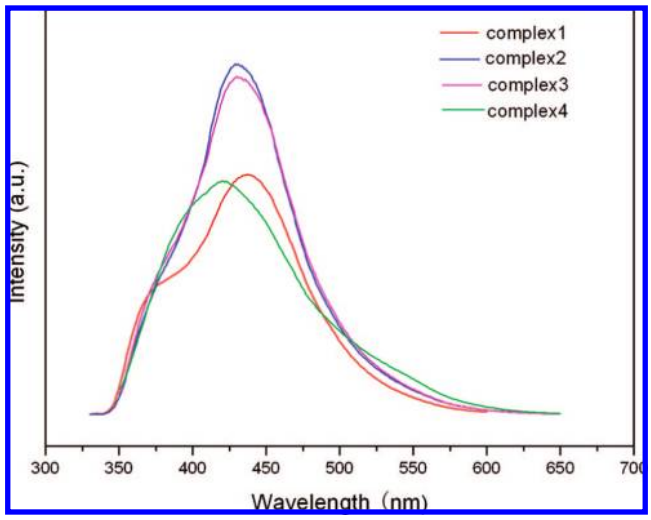

Figure 9. Fluorescence emission spectra of **1**–**4** in solid state.

through the threading of oba arms. It differs from **4** in that the nodes are represented by both the single Ni centers and the binuclear $[Ni_2(COO)_4]$ units arranged alternately within a flat (4, 4) layer and in that every rhombic window is threaded by only two dangling arms because the dangling oba ligands are only coordinated to the binuclear units.

Thermal Stability and Fluorescent Properties. Complexes **1**–**4** were subjected to thermogravimetric analysis (TGA) to ascertain the stability of their respective supramolecular architectures (see the Supporting Information). For complex **1**, the weight loss corresponding to the release of water molecules is observed from 40 to 220 °C, showing good stability due to the existence of tetrameric water clusters in the channels, whereas complex **2** loses its water molecules at about 115 °C. Decomposition of organic components occurs at 263 and 259 °C for **1** and **2**, respectively, and both compounds exhibit a similar decomposing process in two steps. Complex **3** loses its water molecules from 40 to 230 °C and the dehydrated sample is stable up to 358 °C, at which the framework begins to collapse. Complex **4** can keep integrity until 223 °C, and then the framework breaks down in three steps. The thermal stability of **1**–**4** is in accord with their structural features: interpenetrated compounds **1** and **2** show similar decomposing temperature and process, and polyrotaxane **3** is more stable than polythreaded **4** because the latter contains a "separable" motif from a topological point of view.

To study the fluorescent properties of these compounds, the emission spectra of **1**–**4** in solid state at ambient temperature were measured (Figure 9). Intense fluorescent emissions at 438 nm (λ_{ex} = 350 nm) for **1**, 430 nm (λ_{ex} = 330 nm) for **2**, 431 nm (λ_{ex} = 333 nm) for **3** and 422 nm (λ_{ex} = 340 nm) for **4** were observed. All the four compounds have similar excitation and emission wavelengths. According to the literature, the H_2tp and bpp ligands exhibit emission bands at 387 nm (λ_{ex} = 262 nm)[25] and 521 nm (λ_{ex} = 400 nm),[26] respectively. Therefore, the emissions of **1**−**4** may be assigned to intraligand fluorescence emission. The enhancement of luminescence for **2** and **3** may be attributed to two chelating tp ligands in the equatorial plane of a pentagonal-bipyramidal metal center. The chelating coordination effectively increases the rigidity of the ligands and reduces the loss of energy by radiationless decay.[27] No chelating ligand is observed in **1**, whereas only one chelating tp ligand binds to an octahedral metal in **4**. This suggests that **2** and **3** may be good candidates for potential hybrid inorganic–organic photoactive materials.

Conclusion

A family of four new coordination polymers have been obtained by a combination of divalent metal ion Zn(II) or Cd(II) with tp and bpp ligands. Although the same starting building blocks and similar synthetic conditions were utilized, the compounds manifest quite different structural architectures. **1** and **2** display different degrees of interpenetration with different topologies. **3** represents a rare example of 2D polyrotaxane network while **4** shows an unusual feature of polythreading. Entangled structures are now becoming increasingly common in the realm of coordination polymers. Our results suggest that novel extended entanglements can be realized by combining metal nodes with rigid ligands such as tp and flexible ligands like bpp. With more complex types of entanglements being discovered, topological study can play a more important role in the crystal engineering of coordination polymers.

Acknowledgment. This work was supported by Changchun Institute of Applied Chemistry, Changchun, P. R. China.

Supporting Information Available: X-ray crystallographic files in CIF format and TGA curves for **1**−**4** (PDF). This information is available free of charge via the Internet at http://pubs.acs.org.

References

(1) For example: (a) Moulton, B.; Zaworotko, M. J. *Chem. Rev* **2001**, *101*, 1629–1658. (b) Leininger, S.; Olenyuk, B.; Stang, P. J. *Chem. Rev.* **2000**, *100*, 853–908. (c) Belanger, S.; Keefe, M. H.; Welch, J. L.; Hupp, J. T. *Coord. Chem. Rev.* **1999**, *190*−*192*, 29–45. (d) Hagrman, P. J.; Hagrman, D.; Zubieta, J. *Angew. Chem., Int. Ed.* **1999**, *38*, 2638–2684. (e) Eddaoudi, M.; Moler, D. B.; Li, H.; Chen, B.; Reineke, T. M.; O'Keeffe, M.; Yaghi, O. M. *Acc. Chem. Res.* **2001**, *34*, 319–330. (f) Evans, O. R.; Lin, W. *Acc. Chem. Res.* **2002**, *35*, 511–522. (g) Kitagawa, S.; Kitaura, R.; Noro, S. *Angew. Chem., Int. Ed.* **2004**, *43*, 2334–2375. (h) James, S. L. *Chem. Soc. Rev.* **2003**, *32*, 276–288. (i) Janiak, C. *Dalton Trans.* **2003**, 2781–2804. (j) Hong, M. *Cryst. Growth Des.* **2007**, *7*, 10–14.

(2) (a) Kumar, D. K.; Das, A.; Dastidar, P. *CrystEngComm* **2006**, *8*, 805–814. (b) Wang, R.; Yuan, D.; Jiang, F.; Han, L.; Gong, Y.; Hong, M. *Cryst. Growth Des.* **2006**, *6*, 1351–1360.

(3) (a) Robson, R. *J. Chem. Soc., Dalton Trans.* **2000**, 3735–3744. (b) Batten, S. R. *J. Solid State Chem.* **2005**, *178*, 2475–2479. (c) O'Keeffe, M.; Eddaoudi, M.; Li, H.; Reineke, T.; Yaghi, O. M. *J. Solid State Chem.* **2000**, *152*, 3–20.

(4) (a) Batten, S. R.; Robson, R. *Angew. Chem., Int. Ed.* **1998**, *37*, 1460–1494. (b) Batten, S. R. *CrystEngComm* **2001**, *3*, 67–72.

(5) (a) Carlucci, L.; Ciani, G.; Proserpio, D. M. *Coord. Chem. Rev.* **2003**, *246*, 247–289. (b) Carlucci, L.; Ciani, G.; Proserpio, D. M. *CrystEngComm* **2003**, *5*, 269–279.

(6) (a) Zhang, J.; Chen, Y. B.; Li, Z. J.; Qin, Y. Y.; Yao, Y. G. *Inorg. Chem. Commun.* **2006**, *9*, 449–451. (b) Zhang, J.; Li, Z. J.; Cao, X. Y.; Yao, Y. G. *J. Mol. Struct.* **2005**, *750*, 39–43. (c) Dai, Y. M.; Ma, E.; Tang, E.; Zhang, J.; Li, Z. J.; Huang, X. D.; Yao, Y. G. *Cryst. Growth Des.* **2005**, *5*, 1313–1315.

(7) (a) Zaworotko, M. J. *Chem. Commun.* **2001**, 1–9. (b) Dai, J. C.; Wu, X. T.; Fu, Z. Y.; Hu, S. M.; Du, W. X.; Cui, C. P.; Wu, L. M.; Zhang, H. H.; Sun, R. Q. *Chem. Commun.* **2002**, 12–13.

(8) *SADABS, Software for Empirical Absorption Correction*, version 2.03; Bruker AXS, Inc.: Madison, WI, 2002.

(9) Sheldrick, G. M. *Acta Crystallogr., Sect. A* **2008**, *64*, 112–122.

(10) (a) Yaghi, O. M.; Davis, C.; Li, H.; Richardson, D.; Groy, T. L. *Acc. Chem. Res.* **1998**, *31*, 474–484. (b) Rao, C. N. R.; Natarajan, S.; Vaidhyanathan, R. *Angew. Chem., Int. Ed.* **2004**, *43*, 1466–1496.

(11) (a) Carlucci, L.; Ciani, G.; Gudenberg, D. W. v.; Proserpio, D. M. *Inorg. Chem.* **1997**, *36*, 3812–3813. (b) Carlucci, L.; Ciani, G.; Moret, M.; Proserpio, D. M.; Rizzato, S. *Angew. Chem., Int. Ed.* **2000**, *39*,

1506–1510. (c) Tabellion, F. M.; Seidel, S. R.; Arif, A. M.; Stang, P. J. *J. Am. Chem. Soc.* **2001**, *123*, 11982–11990. (d) Chen, P. K.; Che, Y. X.; Xue, L.; Zheng, J. M. *Cryst. Growth Des.* **2006**, *6*, 2517–2522.

(12) Blatov, V. A.; Carlucci, L.; Ciani, G.; Proserpio, D. M. *CrystEngComm* **2004**, *6*, 378–395.

(13) O'Keeffe, M.; Brese, N. E. *Acta Crystallogr., Sect. A* **1992**, *48*, 663–669.

(14) Spek, A. L. *PLATON, A Multipurpose Crystallographic Tool*; Utrecht University: Utrecht, The Netherlands, 1998.

(15) (a) Zuhayra, M.; Kampen, W. U.; Henze, E.; Soti, Z.; Zsolnai, L.; Huttner, G.; Oberdorfer, F. *J. Am. Chem. Soc.* **2006**, *128*, 424–425. (b) Li, Z.-G.; Xu, J.-W.; Jia, H.-Q.; Hu, N.-H. *Inorg. Chem. Commun.* **2006**, *9*, 969–972.

(16) Montney, M. R.; Krishnan, S. M.; Patel, N. M.; Supkowski, R. M.; LaDuca, R. L. *Cryst. Growth Des.* **2007**, *7*, 1145–1153.

(17) Wang, X.-W.; Dong, Y.-R.; Zheng, Y.-Q.; Chen, J.-Z. *Cryst. Growth Des.* **2007**, *7*, 613–615.

(18) (a) Kuehl, C. J.; Tabellion, F. M.; Arif, A. M.; Stang, P. J. *Organomet.* **2001**, *20*, 1956–1959. (b) Fraser, C. S. A.; Jennings, M. C.; Puddephatt, R. J. *Chem. Commun.* **2001**, 1310–1311.

(19) (a) Hoskins, B. F.; Robson, R.; Slizys, D. A. *J. Am. Chem. Soc.* **1997**, *119*, 2952–2953. (b) Carlucci, L.; Ciani, G.; Proserpio, D. M. *Cryst. Growth Des.* **2005**, *5*, 37–39.

(20) Hoskins, B. F.; Robson, R.; Slizys, D. A. *Angew. Chem., Int. Ed. Engl.* **1997**, *36*, 2336–2338.

(21) (a) Lin, P.; Clegg, W.; Harrington, R. W.; Henderson, R. A.; Fletcher, A. J.; Bell, J.; Thomas, K. M. *Inorg. Chem.* **2006**, *45*, 4284–4302. (b) Zhang, J.; Chen, Y. B.; Chen, S. M.; Li, Z. J.; Cheng, J. K.; Yao, Y. G. *Inorg. Chem.* **2006**, *45*, 3161–3163. (c) Liu, Q. Y.; Wang, Y. L.; Xu, L. *Eur. J. Inorg. Chem.* **2006**, 4843–4851.

(22) Carlucci, L.; Ciani, G.; Proserpio, D. M. *Chem. Commun.* **1999**, 449–450.

(23) Tong, M.-L.; Chen, H.-J.; Chen, X.-M. *Inorg. Chem.* **2000**, *39*, 2235–2238.

(24) Wang, X.-L.; Qin, C.; Wang, E.-B.; Li, Y.-G.; Su, Z.-M.; Xu, L.; Carlucci, L. *Angew. Chem., Int. Ed.* **2005**, *44*, 5824–5827.

(25) Yang, E.-C.; Zhao, H.-K.; Ding, B.; Wang, X.-G.; Zhao, X.-J. *Cryst. Growth Des.* **2007**, *7*, 2009–2015.

(26) Wen, Y.-H.; Zhang, J.; Wang, X.-Q.; Feng, Y.-L.; Cheng, J.-K.; Li, Z.-J.; Yao, Y.-G. *New J. Chem.* **2005**, *29*, 995–997.

(27) (a) Zheng, S.-L.; Yang, J.-H.; Yu, X.-L.; Chen, X.-M.; Wong, W.-T. *Inorg. Chem.* **2004**, *43*, 830–838. (b) Wei, K.-J.; Xie, Y.-S.; Ni, J.; Zhang, M.; Liu, Q.-L. *Cryst. Growth Des.* **2006**, *6*, 1341–1350. (c) Valeur, B. *Molecular Fluorescence: Principles and Applications;* Wiley-VCH: Weinheim, Germany, 2002.

CG701232N